Metal–insulator transition in *a*-GaSb:Cu

V. V. Brazhkin, S. V. Demishev, Yu. V. Kosichkin, A. G. Lyapin, N. E. Sluchanko,
S. V. Frolov, and M. S. Sharambeyan

Institute of General Physics, Russian Academy of Sciences; L. F. Vereshchagin Institute of High-Pressure Physics, Russian Academy of Sciences

The effect of a copper impurity on the structure and properties of bulk amorphous samples of gallium antimonide synthesized by quenching from the melt at high pressure is investigated. The structure of the *a*-GaSb:Cu samples and their crystallization temperature and heat of crystallization are determined. It is found that the addition of copper during synthesis leads to a progressive change in the structure of the samples as the copper concentration x_{Cu} increases. First, in the interval $0 \leqslant x_{Cu} \leqslant 10$ at.%, the residual crystalline inclusions and regions of nonstoichiometric composition vanish, and then, for $x_{Cu} \geqslant 10$ at.%, the solubility limit of copper in the amorphous matrix *a*-GaSb is reached, and the excess copper precipitates in the form of inclusions of a crystalline intermetallide phase Ga_4Cu_9, which has a much lower conductivity than the amorphous matrix. It is shown that these phase transformations induce a metal–insulator transition in *a*-GaSb:Cu at $x_{Cu} \approx 10$ at.%, which is accompanied by a change in the electrical conductivity by a factor of 10^6, while at $x_{Cu} \approx 32$ at.% percolation via the Ga_4Cu_9 phase sets in, and the resistance of the system drops sharply (insulator–metal transition). The existence of a Hall anomaly, consisting in the resonant increase in the Hall coefficient at the percolation threshold, is observed; this can serve as experimental confirmation of the Shklovskiĭ theory. It is found that besides causing changes in the phase composition, doping also has a substantial effect on the characteristics of the amorphous matrix *a*-GaSb. Based on an analysis of the concentration dependence of the resistivity, mobility, and Hall and Seebeck coefficients, a model is proposed for describing the mechanism of doping of the amorphous phase.

1. INTRODUCTION

Developments in the technique of synthesizing materials under pressure in the past decade have presented experimental solid state physicists with a multitude of new objects of study, such as bulk semiconductors with tetrahedral short-range coordination (CdSb, ZnSb),[1] including diamond lattice A^3B^5 semiconductors (GaSb).[2,3] Such objects are of interest because they undergo a nontrivial sequence of phase transitions as the external conditions (pressure, temperature) are changed: from a crystalline high-pressure phase (metal), to an amorphous semiconductor, to a crystalline semiconductor. It thus becomes possible to study the mechanisms of amorphization in these materials, which differ substantially from the normal glass-forming processes.

Two aspects should be particularly stressed in view of their importance to experimental research on materials of this class. First, amorphization of these materials is a process in the course of which, by varying the p–T parameters of the transformation, one can obtain phase mixtures of a specified composition, from a crystalline metastable high-pressure phase to a completely disordered A^3B^5 compound.

By controlling the composition of the mixture in these materials one can study the details of the amorphization process and create greater opportunities for elucidating the behavior of physical objects consisting of a complex set of phase mixtures.

Another aspect that substantially simplifies the problem of obtaining the necessary set of physical characteristics of an amorphous material as an object of study is that amorphous materials synthesized under pressure are bulk materials, unlike the amorphous A^3B^5 films obtained by deposition on a substrate. It thus becomes possible to work with bulk amorphous A^3B^5 semiconductors and phase mixtures based on them. By analogy with amorphous films, one can expect that the addition of a "doping" element to the amorphous matrix will afford additional possibilities for controlling the physical parameters of pressure-synthesized amorphous materials. While at relatively low impurity concentrations (of a few atomic percent) one can speak of doping in a proper sense and of the resulting changes in the electronic properties, as the impurity concentration is increased the impurity begins to play the role of a structure-forming element. The best-known example of this is amorphous hydrogenated silicon *a*-Si:H, in which the hydrogen concentration can reach 60 at.%.[4] With systems of this kind (and, in particular, *a*-Si:H) it is unclear from a fundamental standpoint whether to regard them as amorphous solid solutions or as multiphase systems.[4]

As far as we know, the problem of doping amorphous semiconductors synthesized by quenching under pressure has never been studied. In this paper we consider the effect of a group-I impurity element (copper) on the structure and properties of bulk samples of amorphous gallium antimonide[2,5] over a wide range of impurity concentrations. The general techniques and conditions for synthesis of the samples and the methods of investigating their physical properties have been described in detail in our previous article.[5]
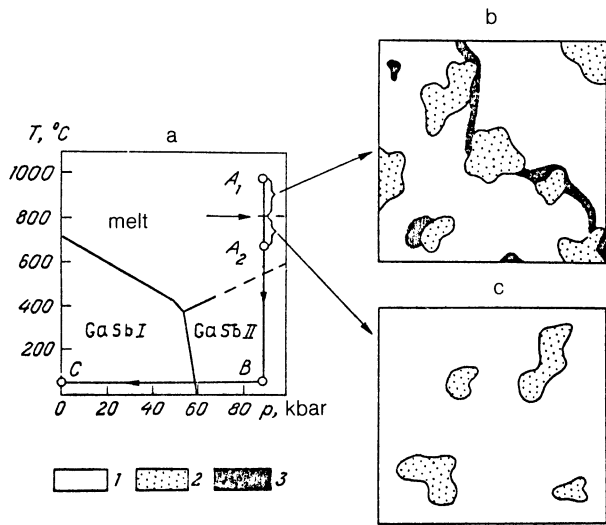
0038-5646/92/061020-09$05.00

FIG. 1. a: The p–T phase diagram of GaSb and the scheme used to synthesize a-GaSb samples by temperature quenching at high pressure; b,c: schematic picture of the phase structure of a-GaSb samples obtained under various conditions, according to the data of Ref. 5: 1) amorphous matrix a-GaSb; 2) crystalline phase c-GaSb; 3) nonstoichiometric amorphous phase $Ga_x Sb_{1-x}$.
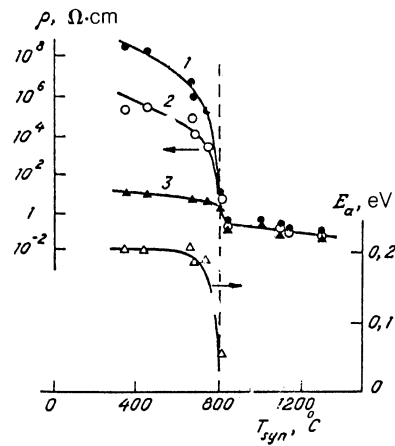

FIG. 2. Dependence on the synthesis temperature T_{syn} of the resistivity measured at various temperatures [$T = 4.2$ (1), 100 (2), and 300 K (3)] and of the activation energy of the resistivity for a-GaSb samples.

2. SYNTHESIS SCHEME AND THE METAL–INSULATOR TRANSITION IN a-GaSb: Cu

The scheme which we used to synthesize the a-GaSb:Cu samples in this study (Fig. 1) is analogous to that used for obtaining stoichiometric amorphous samples of a-GaSb. In the case of a stoichiometric composition the initial crystalline sample of GaSb is first subjected to high pressure (above the pressure of the phase transition GaSb I→II) and high temperature (point A on the p–T phase diagram) and is then quenched to room temperature (point B). After the pressure is removed (point C) the high-pressure phase GaSb II, which has the β-Sn structure and is metastable under normal conditions, goes over to an amorphous phase with tetrahedral coordination of the bonds and a short-range ordered structure that corresponds to the semiconducting phase GaSb I (Ref. 5).

It was found previously[5] that the structure and properties of the a-GaSb samples thus obtained depend in a complicated way on the synthesis conditions, even in the case of pure gallium antimonide. Therefore, before turning to a description of how the copper introduced during synthesis affects the physical properties of a-GaSb, let us discuss the known results for the undoped case.

According to Ref. 5, the most important parameter determining the properties of a-GaSb samples is the synthesis temperature T_{syn}. If the parameter T_{syn} is less than a certain critical value T^*_{syn} ($T^*_{syn} \approx 800$ °C at $p = 90$ kbar), the structure of the a-GaSb samples consists of an amorphous matrix a-GaSb containing inclusions of the crystalline phase c-GaSb. The fraction of c-GaSb by volume is small and can be estimated as $n_c \sim 5$–10%, the value of n_c increasing with T_{syn} (Ref. 5).

Since there is no percolation via the crystalline phase, the electrical conductivity of the system is determined by

that of the amorphous matrix, which has an activational temperature dependence. The activation energy E_a of the resistivity in the region $T_{syn} < T^*_{syn}$ is practically independent of T_{syn} (Fig. 2) and has the value $E_a \approx 0.18$ eV (Ref. 5).

When the synthesis temperature exceeds the critical value T^*_{syn} the nature of the temperature dependence of the resistivity $\rho(T)$ changes substantially: the activational behavior $\rho \propto \exp(E_a/kT)$ goes over to a quasi-metallic behavior $\rho(T) \approx$ const, and in the temperature range $2 \leqslant T \leqslant 10$ K the a-GaSb samples exhibit a diffuse superconducting transition.[5] From the $\rho(T_{syn})$ data measured at various temperatures (Fig. 2) it is seen that the value of ρ measured at $T = 4.2$ K can change by a factor of 10^8–10^9 at the metal-insulator transition induced by a change in T_{syn}.

According to Ref. 5, the metal–insulator transition in a-GaSb is due to the appearance of metallic superconducting inclusions of nonstoichiometric composition, with a characteristic dimension of ~ 200 Å, in the a-GaSb matrix in addition to the crystalline clusters of c-GaSb. The formation of these metallic inclusions of a-GaSb at high synthesis temperatures $T_{syn} > 800$ °C (see Fig. 1) is apparently due to dissociation of the components in the GaSb melt as the temperature of the melt increases.[6] Cooling of such a melt with subsequent removal of the pressure leads to quenching of nonstoichiometric inclusions of $Ga_x Sb_{1-x}$, which have metallic conductivity, in the volume of the semiconducting amorphous phase. Lowering the synthesis temperature to $T_{syn} < 800$ °C (the insulator side of the metal–insulator transition) prevents dissociation of the GaSb melt, so that the "network" of metallic channels in the a-GaSb does not form.[5]

Analysis of the superconducting properties of a-GaSb shows that the concentration of the $Ga_x Sb_{1-x}$ is not more than a few percent,[5] so that in order to bring about a resistive transition ($\rho = 0$) the superconducting phase must be limited to filamentary structures which, together with the inclusions of the crystalline phase, shunt the high-resistivity amorphous matrix (for $T_{syn} > 800$ °C the content of the crystalline phase reaches $x_c \sim 15$–17%).

The structure of the a-GaSb samples synthesized at $T_{syn} > 800\,°C$ and $T_{syn} < 800\,°C$ are shown schematically in Fig. 1.

To ensure a uniform distribution of copper in the a-GaSb:Cu samples in the synthesis scheme used (Fig. 1) it was necessary to heat the samples to temperatures above T^*_{syn}. In this case the samples of the system a-GaSb:Cu with zero copper content, $x_{Cu} = 0$, have the structure shown schematically in Fig. 1b and possess superconducting properties due to the presence of the $Ga_x Sb_{1-x}$ phase.

Now let us consider the evolution of the phase composition of a-GaSb:Cu samples as x_{Cu} is increased and the resulting changes in the physical properties of this complex multiphase system. All the samples were synthesized under the same conditions, $P_{syn} = 90$ kbar, $T_{syn} = 1100\,°C$, while the copper content varied in the range $0 \leqslant x_{Cu} \leqslant 47$ at.%.

It was found that increasing the copper concentration x_{Cu} leads to a substantial change in the conductivity of the a-GaSb:Cu samples (Fig. 3). Initially, for concentrations in the region $x_{Cu} \approx 3$ at.%, the superconductivity is inhibited (curves 1 and 2 in Fig. 3), with the resistivity in the region $T > 10$ K remaining practically unchanged, and then ρ begins to increase as x_{Cu} is increased further (curve 3–6 in Fig. 3), and in the region $x_{Cu} \approx 10$ at.% the quasi-metallic behavior $\rho(T) \approx$ const gives way to an activational dependence, with an activation energy $E_a \approx 0.17$–0.19 eV. Note that this value of E_a is in good agreement with the data previously obtained[5] for an undoped sample of a-GaSb synthesized at $T_{syn} < T^*_{syn}$.

The growth trend of $\rho(x_{Cu})$ continues all the way to values $x_{Cu} \approx 27$ at.% (curve 6 in Fig. 3), after which the resistivity of the a-GaSb:Cu system decreases sharply (curves 7 and 8 in Fig. 3), and in the region $x_{Cu} \approx 50$ at.% it stabilizes at a level $\rho \approx 2 \times 10^{-3}$ $\Omega \cdot$cm. Then the semiconductor behavior of $\rho(T)$ again gives way to a metallic behavior.

Interestingly, the increase in ρ as the copper content is changed is by a factor of $\sim 10^6$, which is about two orders of magnitude smaller than in the case of the metal–insulator
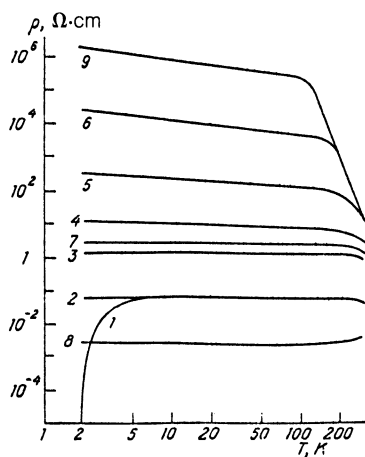
transition occurring in a-GaSb due to a change in T_{syn} (see Fig. 3; curve 9 corresponds to an undoped a-GaSb sample obtained at $T_{syn} < T^*_{syn}$).

Thus the changes in x_{Cu} in a-GaSb:Cu induce first a metal–insulator transition and then an insulator–metal transition. To explain the nature of such a transformation of the electronic properties of a-GaSb:Cu requires examination of the structural analysis data.

3. STRUCTURE OF THE a-GaSb:Cu SAMPLES

Let us first analyze the data from x-ray structure measurements. Figure 4 shows the scattering structure factors $a(s)$ obtained by isolating the coherent part of the x-ray scattering intensity curves $I(s)$ for several of a series of a-GaSb:Cu samples. It is seen that the samples with low copper content ($x_{Cu} \leqslant 15$ at.%), like the undoped a-GaSb, retain a small amount of the crystalline phase of GaSb. An estimate of the concentration n_c of the external phase in samples of the a-GaSb:Cu system by the correlation technique for analysis of the composition of phase mixtures[5] gave a value $n_c \approx 15\%$, in agreement with the data for undoped a-GaSb. The significant broadening of the peaks corresponding to the GaSb crystal for samples in this range of concentrations x_{Cu} (curves 1, lines a in Fig. 4) in comparison with the scattering from an unstressed single crystal indicates that the crystallites are small, ~ 100–300 Å.

Increasing the copper concentration further leads to the following changes in the structure of the a-GaSb:Cu samples. In the region $x_{Cu} \approx 10$ at.% the crystalline lines of c-GaSb (the set of a lines in Fig. 4) disappear, and a new line appears in the neighborhood of $s \approx 3$ Å (curves 2 and 3, line b in Fig. 4), corresponding to inclusions of a new crystalline phase that is different from c-GaSb.

Increasing x_{Cu} in the range $x_{Cu} \geqslant 10$ at.% leads to sharp growth in the amplitude of the new line, and for $x_{Cu} \geqslant 20$ at.% various ancillary lines begin to appear in addition to the main intensity peak at $s \approx 3$ Å (curve 3 in Fig. 4). This circumstance has permitted identification of the new phase: this set of lines in the region $x_{Cu} \geqslant 10$ at.% corresponds to inclusions of the intermetallide Ga_4Cu_9 (Ref. 7).

We see from Fig. 4 that in addition to the contribution from inclusions of Ga_4Cu_9, the structure factors $a(s)$ exhibit broad maxima corresponding to the amorphous phase a-GaSb over the entire investigated range of concentrations x_{Cu}. Let us now discuss how doping with copper influences the structure of the a-GaSb itself.

For the $a(s)$ spectra (Fig. 4) we isolated the contributions corresponding to the amorphous phase a-GaSb, which were then used to calculate the radial distribution functions of the atomic density and to estimate the correlation length L_c. The radial distribution functions of a-GaSb:Cu were calculated by the usual approach for multicomponent systems.[8] The coordinate of the first peak of the radial distribution functions for samples of the system a-GaSb:Cu, $R_1 = 3.17 \pm 0.1$ Å, remained unchanged to within the experimental accuracy as the copper content was varied. The behavior of the coordination number $z_1(x_{Cu})$ calculated from the radial distribution functions is plotted by curve 1 in Fig. 5a. The parameter z_1, which corresponds to the number of nearest neighbors in the structure a-GaSb:Cu, initially decreases smoothly from 3.71 ($x_{Cu} = 0$) to 3.66 ($x_{Cu} \approx 17$

FIG. 3. Temperature dependence of the resistivity of a-GaSb:Cu samples with various compositions x_{Cu}: 1) $x_{Cu} = 0$ (undoped sample, $T_{syn} > T^*_{syn}$); 2) 3 at.%; 3) 11 at.%; 4) 14 at.%; 5) 18 at.%; 6) 27 at.%; 7) 31 at.%; 8) 47 at.%. The curve of $\rho(T)$ for an undoped a-GaSb sample obtained at $T_{syn} < T^*_{syn}$ is shown for comparison (curve 9).
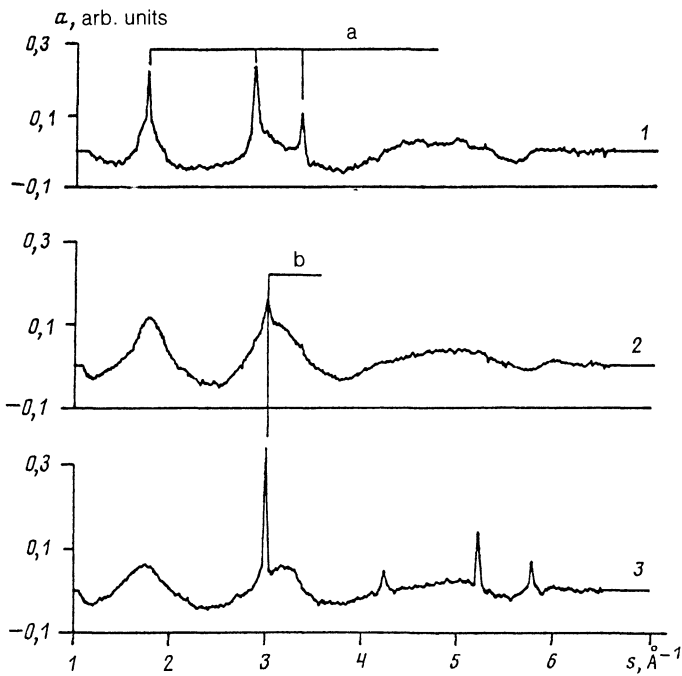
FIG. 4. Structure factor for x-ray scattering (CuK_α line, $\lambda = 1.5418$ Å) for a-GaSb samples with various Cu contents: *1*) $x_{Cu} = 7$ at.%; *2*) 11 at.%; *3*) 27 at.%; $s = (4\pi/\lambda)\sin\theta$. a: the crystalline lines of c-GaSb; b: the lines of Ga_4Cu_9.

at.%), and then at $x_{Cu} \geqslant 17$ at.% it falls to 3.61 and stabilizes near this value for copper concentrations $x_{Cu} \geqslant 20$ at.%. In calculating the radial distribution functions we used the densities of the a-GaSb:Cu samples given in Fig. 5c. It is seen that the region of smooth decrease in the coordination number corresponds to concentrations $x_{Cu} < 20$ at.%, where the pycnometric density of the samples remained unchanged ($\rho \approx 5.56$ g/cm^3).

Note that this anomaly in $z_1(x_{Cu})$ is evidently not due to the appearance of Ga_4Cu_9 inclusions in the volume of the sample, since the decrease in the relative amplitude $I(s)$ for the first amorphous peak, due to inclusions, in the structure

FIG. 5. Concentration dependence of: a) the coordination number z_1 (*1*) and the amplitude of the first peak for a-GaSb:Cu (*2*); b) the correlation length L_c; c) the pycnometric density ρ_0; d) the microhardness σ of a-GaSb:Cu samples (the dark triangle corresponds to a sample obtained at $T_{syn} < T_{syn}^*$, having the minimum content of the crystalline phase).

factor $a(s)$ begins at $x_{Cu} \approx 10$ at.% (curve *2* in Fig. 5a) and not at $x_{Cu} \approx 17$ at.%, as in the case of $z_1(x_{Cu})$ (curve *1* in Fig. 5a).

Another important characteristic of the amorphous phase of a-GaSb:Cu is the correlation length L_c, which characterizes the spatial dimensions of the regions in which the short-range order of the structure is preserved. The parameter L_c was calculated by the formula[9]

$$L_c = 0{,}9\lambda/\Delta(2\theta)\cos\theta_0, \qquad (1)$$

where λ is the wavelength of the x rays and θ_0 and $\Delta(2\theta)$ are the coordinate and half-width (at the half amplitude level) of the first amorphous peak. The estimates thus obtained indicate that the average size of the coherent-scattering regions of the amorphous matrix for the a-GaSb:Cu phase falls off linearly with increasing x_{Cu} over the entire range of investigated concentrations (Fig. 3b). We note that $L_c(x_{Cu} = 0) \approx 6.1$ Å, which is close to twice the lattice constant of gallium antimonide.

Thus the x-ray structure data suggest the following picture of phase transformations in the a-GaSb:Cu system and the resulting morphological changes in the samples. Initially ($x_{Cu} \leqslant 10$ at.%) the introduction of copper causes the crystalline inclusions in the a-GaSb matrix to disappear. It can be assumed that in this stage the copper, being incorporated into the GaSb lattice, plays the role of an "amorphizer," i.e., an agent that facilitates the disordering of the gallium antimonide structure. Indeed, if the copper atoms are regarded as defects of the disordered a-GaSb lattice, one would expect that they will cause additional distortion of the bond lengths and angles, i.e., additional disordering of the system. Such behavior can be manifested in changes in the short-range order (in the average coordination number z_1) and in the intermediate order (the correlation length L_c), as is indeed observed experimentally (Fig. 5a,b).

In the region $x_{Cu} > 10$ at.% a qualitative rearrangement of the phase state of the a-GaSb:Cu samples occurs: the

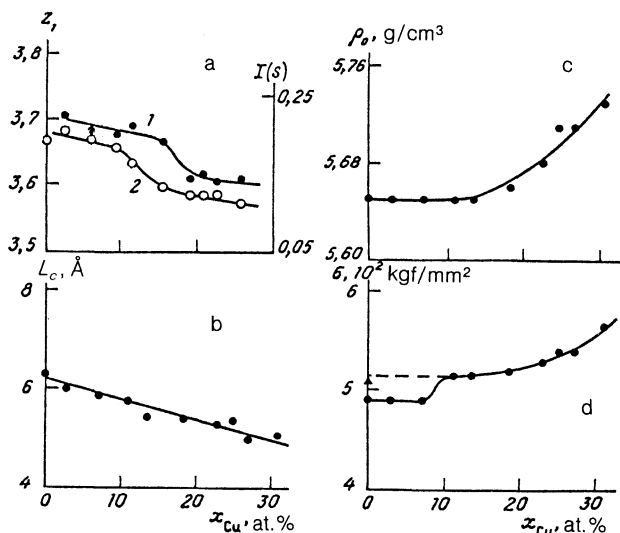*c*-GaSb inclusions vanish and inclusions of the intermetallide Ga_4Cu_9 appear in their place. Most likely the "solubility limit" of copper in the amorphous phase *a*-GaSb is reached at $x_{Cu} \approx 10$ at.%, and the excess copper begins to bind gallium and to precipitate in the form of Ga_4Cu_9 inclusions. As x_{Cu} further increases the fraction of the sample volume occupied by the Ga_4Cu_9 phase increases, but no other qualitative morphological changes occur in the system, according to the x-ray structure data.

It must be emphasized that changes in the characteristics of the amorphous phase *a*-GaSb:Cu itself occur over the entire range of x_{Cu} investigated (Fig. 5a,b), although these changes should apparently be qualitatively different above the "solubility limit" than in the case $x_{Cu} \leqslant 10$ at.%. While for $x_{Cu} \leqslant 10$ at.% the copper is incorporated into the disordered lattice of *a*-GaSb, for $x_{Cu} > 10$ at.% the formation of inclusions of the Ga_4Cu_9 phase begins to dominate. From the standpoint of the amorphous matrix, the removal from it of the gallium atoms used in the formation of Ga_4Cu_9 will give rise to vacancies in the gallium sublattice while the concentration of copper atoms in the amorphous phase *a*-GaSb:Cu remains constant. It is natural to suppose that this mechanism of defect formation will give rise to a large number of broken bonds, and this is manifested in the decreasing trend of the coordination number z_1. We note that if the vacancy concentration exceeds a certain limit, then one would expect relaxation of the short-range structure of the disordered lattice, with a sharp increase in the first coordination number. We assume that it is just such a process that is responsible for the sharp change in z_1 at $x_{Cu} \approx 17$ at.% (curve *1* in Fig. 5a).

The above picture of the phase transformations in the *a*-GaSb:Cu samples is also confirmed by a study of the concentration dependence of the microhardness $\sigma(x_{Cu})$ (Fig. 5d). It is seen that $\sigma(x_{Cu})$ has a jump at $x_{Cu} \approx 10$ at.% and then increases monotonically. In the region $x_{Cu} > 10$ at.% the growth of the microhardness is naturally attributed to the appearance of harder and denser metallic inclusions in the volume of the sample. We note that the region of smooth growth of $\sigma(x_{Cu})$ correlates well with the region in which the density of the *a*-GaSb:Cu samples grows (Fig. 5c).

The jump in $\sigma(x_{Cu})$ at $x_{Cu} \approx 10$ at.% can be attributed to the vanishing of the crystalline inclusions *c*-GaSb and the associated interphase boundaries, which can play the role of "weak links" that limit the strength characteristics of multiphase systems.[10]

If this hypothesis is correct, the amplitude of the jump in σ in the system *a*-GaSb:Cu should correspond to the change in microhardness as the crystalline gallium antimonide content varies in the case $x_{Cu} = 0$. It is seen from Fig. 5d that the value of σ for an *a*-GaSb sample with $x_{Cu} = 0$ that was obtained at $T_{syn} < T^*_{syn}$ and contains the minimum crystalline phase content, on the order of a few percent (the solid triangle in Fig. 5d), lies practically on the extrapolation of the curve of $\sigma(x_{Cu} > 10$ at.%) to $x_{Cu} = 0$ (the dashed line in Fig. 5d). We note that the initial crystalline fraction in the *a*-GaSb:Cu samples is $\approx 15\%$.

Thus the set of experimental data in Fig. 5 confirms the above model of the change in the structure and phase composition of *a*-GaSb:Cu samples on doping with copper. However, these data give no information about the effect of impurity copper on the nonstoichiometric amorphous phase
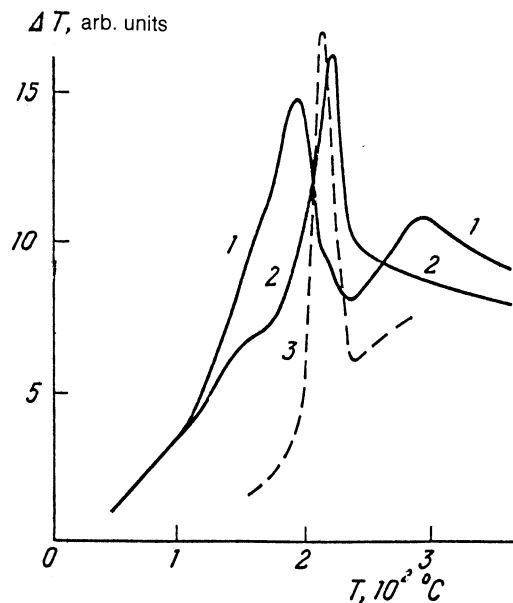

FIG. 6. Differential thermal analysis (DTA) data for samples of *a*-GaSb and *a*-GaSb:Cu. The $\Delta T(T)$ curves for: *1*) *a*-GaSb, $T_{syn} > T^*_{syn}$; *2*) *a*-GaSb, $T_{syn} < T^*_{syn}$; *3*) *a*-GaSb:Cu, $x_{Cu} = 31$ at.% ($T_{syn} > T^*_{syn}$). The temperature scanning rate was 10 deg/min.

$Ga_x Sb_{1-x}$ (see Fig. 1a), since the concentration of this phase is too small to be detected by the x-ray structural analysis techniques at our disposal.[5]

To elucidate this question we performed differential thermal analysis (DTA) on *a*-GaSb:Cu samples and also on samples of *a*-GaSb with $x_{Cu} = 0$, obtained at $T_{syn} > T^*_{syn}$ and $T_{syn} < T^*_{syn}$. The experimental data on $\Delta T(T)$ are shown in Fig. 6.

Let us first discuss the substantial difference in the shapes of the DTA curves for the undoped samples of *a*-GaSb obtained at $T_{syn} > T^*_{syn}$ (curve *1* in Fig. 6) and $T_{syn} < T^*_{syn}$ (curve *2*). When the synthesis temperature exceeds the critical value T^*_{syn} there is not only a broadening of the main heat-release peak, with a shift to lower temperatures, but also an additional maximum appearing in the vicinity of $T \approx 300$ °C. Since the only qualitative difference in the structure of the *a*-GaSb samples obtained at $T_{syn} > T^*_{syn}$ and $T_{syn} < T^*_{syn}$ is the presence of a nonstoichiometric phase $Ga_x Sb_{1-x}$ (see Ref. 5 and also Fig. 1), these features of the DTA curves can be used to identify the presence of this phase in *a*-GaSb samples.

Interestingly, the nonstoichiometric inclusions give contributions in two different temperature intervals. This is an indicator of the presence of dispersion of the structural properties of the $Ga_x Sb_{1-x}$ phase, whose properties can be different for $x > 0.5$ (excess gallium) and $x < 0.5$ (excess antimony), for example.

Let us now discuss the effect of impurity copper on the DTA data. It was found that the introduction of even small amounts of copper ($x_{Cu} \approx 3$ at.%) leads to a decrease in the width of the main heat-release peak. In this same range of concentrations the feature in ΔT at $T \approx 300$ °C is completely suppressed.

The evolution of the DTA curves as the concentration x_{Cu} is increased further consists in a shift in the absolute maximum of the heat release to higher temperatures at a rate of about 0.4 deg/at.% relative to the initial value $T(x = 0) \approx 200\,°C$. The width of the heat-release zone ($\Delta T \approx 60\,°C$) and the heat of crystallization ($\Delta H \approx 12.5$ kJ/mole) remain unchanged.

Consequently, the nonstoichiometric phase $Ga_x Sb_{1-x}$ does not form even in the region $x_{Cu} \geqslant 3$ at.%; this is exhibited in an effective suppression of superconductivity in the a-GaSb:Cu system (Fig. 3).

The microscopic mechanism of this suppression remains unclear. Possibly it is a manifestation of processes in which the copper binds excess gallium (inclusions of $Ga_x Sb_{1-x}$ with $x > 0.5$), similar to those discussed above for the region $x_{Cu} > 10$ at.% and which led to the formation of intermetallic phases. However, it cannot be concluded that the introduction of copper in the synthesis stage has a radical effect on the structure of the GaSb melt, so that the congruent nature of the melting (without dissociation of the components) is maintained up to $T_{syn} \approx 1100\,°C$, and nonstoichiometric inclusions of $Ga_x Sb_{1-x}$ do not form as the melt is quenched. The detailed investigation of this problem is a subject for further studies.

4. EFFECT OF A COPPER IMPURITY ON THE GALVANOMAGNETIC AND THERMOELECTRIC PROPERTIES OF a-GaSb

Using the data on the structure of the a-GaSb:Cu samples obtained in the preceding section, we can now turn to an analysis of the effect of impurity copper on the electrophysical, galvanomagnetic, and thermoelectric phenomena, including identification of the causes of the metal–insulator and insulator–metal transitions in this system. With this goal, let us consider the concentration dependence of the resistivity $\rho(x_{Cu})$, Hall coefficient $R_H(x_{Cu})$, Hall mobility $\mu_H(x_{Cu})$, and Seebeck coefficient $S(x_{Cu})$ (Fig. 7).

First of all let us delineate the characteristic intervals of the parameter x_{Cu} in which the structure or physical properties of a-GaSb:Cu samples change: region I ($0 \leqslant x_{Cu} \leqslant 10$ at.%), region II ($10 \leqslant x_{Cu} \leqslant 32$ at.%), and region III ($x_{Cu} \geqslant 32$ at.%) (see Fig. 7). The transition from region I to region II is characterized by a change in the structure of the samples: the two-phase mixture of amorphous and crystalline phases GaSb I goes over to a different two-component mixture in which inclusions of the intermetallide Ga_4Cu_9 exist in an a-GaSb:Cu matrix.

The boundary between regions II and III is identified by the sharp change in the resistivity (Fig. 7a), corresponding to an insulator–metal transition. The structure of the samples in regions II and III is not qualitatively different (see Sec. 3).

Since the fraction of the sample volume that is occupied by the metallic phase Ga_4Cu_9 in regions II and III increases with increasing x_{Cu}, it is natural to attribute the insulator–metal transition to the onset of percolation via the system of metallic inclusions of Ga_4Cu_9, whose resistivity ρ_m is substantially smaller than the resistivity ρ_d of the amorphous matrix of a-GaSb:Cu.

It is also easy to interpret the metal–insulator transition (the transition from region I to region II), at which the in-
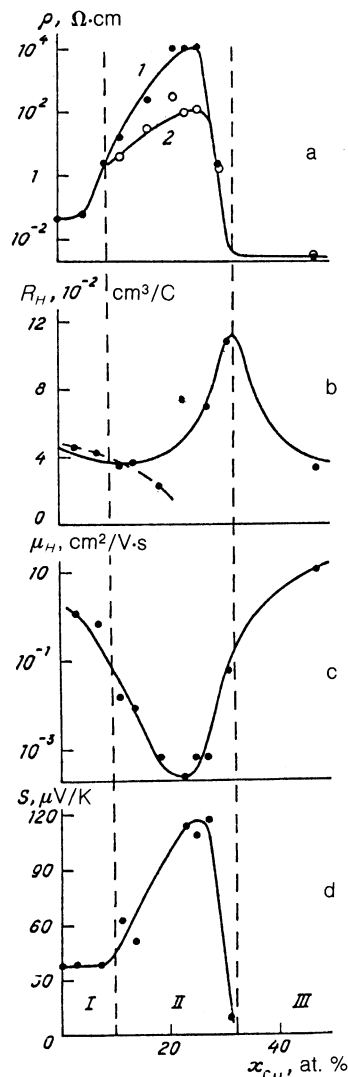

FIG. 7. Concentration dependence of: a) the resistivity $\rho(T, x_{Cu})$ ($T = 4.2$ K, curve 1; $T = 300$ K, curve 2); b) the Hall coefficient $R_H(x_{Cu}, 300$ K); c) the Hall mobility $\mu_H(x_{Cu}, 300$ K); d) the Seebeck coefficient $S(x_{Cu}, 300$ K) for a-GaSb:Cu samples. In part b the solid curve is a model calculation by formula (3) in the framework of the Shklovskiĭ theory, and the dashed curve is the change in R_H as a result of doping of the amorphous matrix.

clusions of the low-resistivity nonstoichiometric amorphous phase $Ga_x Sb_{1-x}$ with $x > 0.5$ first vanish and then, for $x_{Cu} \approx 10$ at.%, the crystalline inclusions also vanish as the copper concentration increases. As a result, the low-resistivity channels that shunt the conductivity of the amorphous matrix in samples obtained at $T_{syn} > T^*_{syn}$ (Ref. 5) do not form, the resistivity increases, and the $\rho(T)$ curves take on the semiconductor behavior that is characteristic of conduction through the amorphous phase a-GaSb (Fig. 3). The superconducting properties of the samples are suppressed even at extremely low concentrations x_{Cu} in region I. It is clear from Fig. 7a that the boundary between regions I and II, which corresponds to a change in the structure of the system, exactly coincides with the metal–insulator transition point (see curves 1 and 2).

The most complex behavior of the a-GaSb:Cu samples occurs in region II, where percolation via the Ga_4Cu_9 phase

is absent and there exists a rather wide interval of concentrations $10 \leqslant x_{Cu} \leqslant 20$ at.% in which the shunting effect of the metallic inclusions is small and the change of the physical properties of the system is determined mainly by the properties of the amorphous phase a-GaSb:Cu itself. The situation here is complicated by the fact that these properties change in region II, i.e., it is necessary to take into account jointly the effect of the metallic inclusions and of the change in the properties of the insulating amorphous matrix.

It follows from Fig. 7a that $\rho(x_{Cu})$ grows strongly (by four orders of magnitude at liquid helium temperature and by two orders of magnitude at room temperature) in region II. We note that if the resistance of the amorphous phase ρ_d remained constant, then the resistivity in this region would not increase with increasing x_{Cu} but would fall off because of the shunting effect of the metallic inclusions with $\rho_m \ll \rho_d$.

Let us consider the behavior of the Hall coefficient R_H in this system (Fig. 7b). Studies made for $T = 300$ K in the field interval $H \leqslant 150$ kOe have shown that the field dependence of the Hall voltage is linear in the accessible range of magnetic fields. It was found that the sign of R_H corresponds to p-type conductivity throughout the investigated concentration range $x_{Cu} \geqslant 0$, in agreement with the data obtained previously[5,11] for undoped samples of a-GaSb.

Note that the concentration dependence $R_H(x_{Cu})$ has a complicated nonmonotonic form: $R_H(x_{Cu})$ initially decreases in the region $x_{Cu} \leqslant 20$ at.%, and then it begins to increase, reaching a maximum at the boundary between regions II and III (the point of the insulator–metal transition, the threshold for percolation via the metallic phase Ga_4Cu_9). As x_{Cu} increases further the Hall coefficient $R_H(x_{Cu})$ decreases (Fig. 7b).

The data on $\rho(x_{Cu})$ and $R_H(x_{Cu})$ (Fig. 7a,b) for $T = 300$ K can be used to calculate the values of the Hall mobility μ_H (Fig. 7c). We see that μ_H decreases by more than four orders of magnitude in the region $0 \leqslant x_{Cu} \leqslant 20$ at.%, reaching a minimum $\mu_H \approx 10^{-4}$ cm^2/V·s at $x_{Cu} \approx 20$ at.%, and then it increases to a value $\mu_H \approx 10$ cm^2/V·s.

The concentration dependence of the Seebeck coefficient $S(x_{Cu})$ is shown in Fig. 7d. The $S(x_{Cu})$ curve practically reiterates the behavior of the resistivity curve $\rho(x_{Cu})$, except that the Seebeck coefficient changes in region II by a factor of two, $S(x_{Cu} = 25$ at.%$)/S(x_{Cu} = 0) = 2$, rather than two orders of magnitude as in the case of the conductivity of the system. The sign of $S(x_{Cu})$ is that of a p-type material.

Let us now consider the experimental results, including the anomalous behavior of the Hall coefficient and the data on the thermo-emf, from the standpoint of the existing theoretical ideas. It is clear that for $x_{Cu} > 10$ at.% (regions II and III) the problem must be treated in a model of an insulating medium containing metallic inclusions. Here, by virtue of the condition $\rho_d \gg \rho_m$, which follows from the data in Fig. 7a, the metallic inclusions can to first approximation be treated as ideally conducting.

The conductivity and the Hall coefficient of such a two-component medium were considered by Shklovskiĭ,[12] and the behavior of the thermo-emf was studied by Skal[13] and Balagurov.[14] Let us assume that the fraction of the volume occupied by the metallic phase, n_m, for a-GaSb:Cu is proportional to x_{Cu}: $n_m = \alpha x_{Cu}$. Then, following Refs. 12–14,

we write the expressions for the effective resistivity and Hall coefficient as

$$\rho \approx \rho_d \tau^q,$$

$$R_H(x_{Cu}) = R_d \tau^{2q} + R_m(\alpha x_c)^{-\nu_3}(\tau^2 + \gamma^2)^{-\nu_3/2} \quad (2)$$

$$= R_H(0)\left(1 - \frac{a}{(1+\gamma^2)^{\nu_3/2}}\right)\tau^{2q} + \frac{a}{(1+\gamma^2\tau^2)^{\nu_3/2}}, \quad (3)$$

where $\tau = 1 - x_{Cu}/x_c$, $a = R_H(x_c)/R_H(0)$, and x_c is the threshold for percolation via the metallic phase. The parameter γ determines the size of the critical region Δ around x_c (the "smearing" region): $\Delta = x_c/\gamma$. The quantities $R_H(0)$ and $R_H(x_c)$ are expressed in terms of the Hall coefficients R_m and R_d of the metal and insulator and the constant α:

$$R_H(x_c) = R_m/(\alpha^2\Delta^2)^{\nu_3/2}, \quad R_H(0) = R_d(\alpha x_c)^{2q} + R_m/(1+\gamma^2)^{\nu_3/2}.$$

As far as we know, the critical exponents q and ν_3 have not been determined experimentally and are not known exactly; a theoretical estimate[12] for the three-dimensional case gives $q \approx 1$, $\nu_3 \approx 0.8$.

The critical behavior of the Seebeck coefficient depends on the ratio between the thermal conductivities $\varkappa_m$ and $\varkappa_d$ of the metal and insulator, respectively. If $\varkappa_m \gg \varkappa_d$, then $S(x_{Cu})$ coincides with S_d almost all the way to x_c, and in a narrow neighborhood of x_c it decreases discontinuously to S_m (S_m and S_d are the thermo-emf of the metal and insulator, respectively). In the case $\varkappa_m \sim \varkappa_d$, the Seebeck coefficient exhibits critical behavior analogous to that of the electrical conductivity:[13,14]

$$S \approx (S_d - S_m)\tau^q + S_m. \quad (4)$$

It follows from Eq. (3) that under certain conditions $R_H(x_{Cu})$ can have a maximum in the neighborhood of the mobility threshold. However, when comparing Eqs. (2)–(4) with experiment it is necessary to keep in mind that in the case of a-GaSb:Cu the parameters ρ_d, R_d, and S_d will also depend on x_{Cu}. For simple estimates we can assume that $R_m = $ const and $S_m = $ const. In addition, it follows from Fig. 7d that $S_d \gg S_m$ holds for a-GaSb:Cu.

It is seen from formulas (2)–(4) that the dependence of the properties of the amorphous matrix a-GaSb:Cu on the copper content has different effects on the behavior of each of the physical quantities describing the system as a whole. The effect is most important in the case of the resistivity ρ and the Seebeck coefficient S, while in the expression for the Hall coefficient the term containing R_d falls off rapidly (as τ^{2q}) as the mobility threshold is approached, and in the percolation region the Hall effect is determined by R_m [see Eq. (3)]. Therefore, in modeling the concentration dependence of $R_H(x_{Cu})$ one can to first approximation set $R_d \approx$ const. One aspect of the calculation in this approximation is that it takes into account only the effect of the inclusions, and therefore the effect of doping of the amorphous phase a-GaSb:Cu can be inferred from the deviation of the experimental points from the theoretical dependence (3).

In order to approximate the experimental data by the formula (3) in the light of these assumptions, it is necessary to know two parameters, a and γ, and the first of these can be estimated directly from the amplitude of the maximum in R_H; for a-GaSb:Cu we get $a \approx 2.5$. Therefore, the only adjus-

table parameter is γ, and the best agreement between the model and experiment is achieved for $\gamma \approx 10$ ($\Delta \approx 0.1 x_c$). It is seen from Fig. 6b (the solid line is the calculation, the points are experimental) that the Shklovskiĭ model[12] correctly conveys the shape of the $R_H(x_c)$ curve over the entire investigated range of copper concentrations, including the presence of a maximum in the Hall coefficient at the percolation threshold.

At the same time, it must be noted that the Hall coefficient falls off more strongly in the region $x_{Cu} \leqslant 20$ at.% than is implied by the approximation (3). This behavior agrees with the model of defect formation in a-GaSb:Cu that was proposed in the preceding section. Indeed, in this region x_{Cu} the concentration of Ga_4Cu_9 inclusions is low, their presence does not have a noticeable shunting effect on the characteristics of the system, and the concentration dependence $R_H(x_{Cu})$ reflects the change in the carrier concentration. According to the assumptions made, the formation of the Ga_4Cu_9 phase is accompanied by the generation of defects of the vacancy type. It is known[15] that in GaSb, vacancies act as a source of p-type carriers, with the result that the hole concentration grows and $R_d(x_{Cu})$ decreases as x_{Cu} increases. Consequently, the experimental points of $R_H(x_{Cu})$ for $x_{Cu} \leqslant 20$ at.% lie below the theoretical curve (Fig. 7b).

Let us now return to discussion of the concentration dependence $\rho(x_{Cu})$ in region II. Our analysis shows that $\rho(x_{Cu})$ increases in spite of the increase in the carrier concentration and the shunting effect of inclusions with metallic conductivity. To explain the reasons for this increase in the resistivity, let us examine the behavior of the mobility $\mu_H(x_{Cu})$.

As expected, in region II, up to $x_{Cu} \approx 20$ at.%, the Hall mobility decreases strongly (by three orders of magnitude). Since the shunting effect of the metallic inclusions is not very large, we hypothesize that this decrease reflects a change in the nature of the scattering in the amorphous phase a-GaSb:Cu. In the percolation region $x_{Cu} \geqslant 20$ at.% the effective mobility increases on account of the gradual transition to conduction via the intermetallic phase Ga_4Cu_9. We note that for $x_{Cu} > x_c$, after an infinite cluster of crystalline inclusions of Ga_4Cu_9 has already formed, the values of the mobility $\mu_H \approx 10$ cm^2/V·s remain rather low, apparently indicating that the Ga_4Cu_9 phase is strongly saturated with defects.

Let us consider the causes of the decrease in mobility and growth of ρ. The x-ray structure data (Fig. 4a,b) imply that the following changes in the structural properties of the amorphous phase a-GaSb:Cu occur in region II: the coordination number z_1 and the correlation length L_c decrease. The change in z_1 can be interpreted as a change in the number of defects of the amorphous lattice, i.e., in the number of scattering centers for current carriers, and a decrease in z_1 corresponds to an increase in the number of scatterers. At the same time, the correlation length L_c characterizes not only the spatial position of the atoms but also determines the spatial scale of the fluctuations of various physical properties in the amorphous medium, particularly of the random potential in which the charge carriers move. Therefore, the decrease in L_c means that the random potential becomes "choppier," and this also enhances the scattering.

Thus the scattering on both localized defects and potential fluctuations should become stronger as x_{Cu} increases; this apparently accounts for the growth in the resistivity of the amorphous matrix. Unfortunately, the data obtained in the present study are insufficient to identify which of the mobility-limiting mechanisms is dominant in a-GaSb:Cu. This question will be the subject of further study.

We conclude this section with an analysis of the relationship between the function $\rho(x_{Cu})$ and $S(x_{Cu})$. According to Ref. 16, if the mobility of the amorphous semiconductor is governed by activation to the mobility threshold, the quantities ρ_d and S_d are connected by the relation

$$\ln(\rho_d \sigma_{min}) = e S_d / k - 1. \qquad (5)$$

where e is the electron charge, k is Boltzmann's constant, $\sigma_{min} = 0.026 \, e^2/\hbar L$ is the minimum metallic conductivity, and L is the characteristic length over which the "memory" of the phase of the wave function of the charge carrier is lost.

It is clear that this conductivity mechanism can occur in samples with the minimum values of the mobility, when the $\rho(T)$ curves exhibit distinct activational segments. To be specific, let us consider a sample with $x_{Cu} = 27$ at.%, for which $\rho(300 \, K) \approx 100 \, \Omega \cdot$cm. Using Eq. (2), we easily find that in this case $\rho_d \approx 640 \, \Omega \cdot$cm.

If the value of S_d is known, then we can easily obtain an estimate of σ_{min} using Eq. (5). Since the relation between S and S_d depends on the relationship between the thermal conductivities $\varkappa_d$ and $\varkappa_m$, let us examine the existing possibilities. If $\varkappa_d \ll \varkappa_m$ and $S \approx S_d$, Eq. (5) gives $\sigma_{min} \approx 2 \times 10^{-3}$ $(\Omega \cdot$cm$)^{-1}$, which corresponds to lengths $L \approx 3 \times 10^{-3}$ cm, which are scarcely possible in an amorphous semiconductor at the mobility edge. In the limit $\varkappa_d \sim \varkappa_m$ Eq. (4) can be used to calculate S_d. For $S_d \gg S_m$ and $S \approx 120 \, \mu V/$deg (Fig. 7d), this gives $S_d \approx 770 \, \mu V/$deg. Using this value, we find $\sigma_{min} \approx 4.3 \, (\Omega \cdot$cm$)^{-1}$ and $L \approx 140$ Å. The latter estimate of σ_{min} agrees with the value of the pre-exponential factor in the activation law for the resistivity $\rho = \rho_0 \exp(E_a / kT)$: according to the data of Fig. 3, in the investigated region of concentrations we have $\rho_0^{-1} \sim \sigma_{min} \sim 2.3$–$5.5 \, (\Omega \cdot$cm$)^{-1}$.

Thus we see that the effect of the metallic inclusions in a-GaSb:Cu is described by the same percolation law for ρ and S, the situation corresponding to the case $\varkappa_d \sim \varkappa_m$. This circumstance, together with relation (5), which is in good agreement with the experimental data, is responsible for the similarity in the behavior of the concentrations $\rho(x_{Cu})$ and $S(x_{Cu})$.

5. CONCLUSION

We have thus determined the sequence of phase transformations arising in bulk samples of amorphous gallium antimonide as a result of the introduction of a copper impurity. If the copper concentration is not too high ($x_{Cu} \leqslant 10$ at.%) a sort of "preamorphization" of a-GaSb occurs, culminating in the disappearance of crystalline inclusions and inclusions of the amorphous nonstoichiometric phase $Ga_x Sb_{1-x}$ in the volume of the sample. The solubility limit of copper in the amorphous matrix a-GaSb is reached at concentrations $x_{Cu} \approx 10$ at.%, and the excess copper begins to form inclusions of the intermetallide Ga_4Cu_9, which have a substantially higher conductivity than a-GaSb:Cu. As x_{Cu} increases, the concentration of these inclusions increases,

and at $x_{Cu} \approx 32$ at.% the inclusions form an infinite cluster.

This sequence of structural changes in the samples determines the nature of the changes in the electrophysical, galvanomagnetic, and thermoelectric properties as x_{Cu} increases. In particular, increasing x_{Cu} induces a metal–insulator transition at $x_{Cu} \approx 10$ at.%, which is due to the vanishing of shunting channels formed by the crystalline phase and inclusions of $Ga_x Sb_{1-x}$. Further increase in x_{Cu} brings on an insulator–metal transition, which is due to the formation of a percolation chain of Ga_4Cu_9 inclusions. We note that this mechanism of doping of noncrystalline materials, wherein the changes in the physical properties occur as a result of changes in the phase composition of the samples, is characteristic for glassy chalcogenide semiconductors.[17]

However, the effect of impurity copper on the properties of a-GaSb:Cu does not reduce solely to a change in the phase composition of the samples. It can be shown that doping leads to changes in the properties of the amorphous matrix. The proposed model, which links the formation of Ga_4Cu_9 inclusions with an increase in the number of defects in the gallium sublattice of the amorphous phase a-GaSb, permits a qualitative description of the whole body of experimental data, although it remains controversial. It can be expected that further studies involving the introduction of impurities with other valences (e.g., Si and Ge)[18] in a-GaSb will make it possible to establish more precisely the microscopic mechanisms of doping of the amorphous matrix.

In analyzing complex multicomponent systems, of which a-GaSb:Cu is an example, it is important to use models based on percolation theory. We have found that percolation theory can describe not only the behavior in the electrical conductivity but also that of the thermo-emf and the Hall coefficient in the neighborhood of the insulator–metal transition. In particular, we have obtained experimental confirmation of the Shklovskiĭ theory, which predicts a peak of the resonance type for the Hall coefficient at the percolation threshold.

As we have seen for the example of amorphous gallium antimonide, doping of new noncrystalline materials synthesized by quenching of the melt at high pressure opens up new possibilities for controlling the physical properties of materials of this class.

[1] E. G. Ponyatovsky, I. T. Belash, and O. I. Barkalov, J. Non-Cryst. Solids **117–118**, 679 (1990).

[2] S. V. Demishev, Yu. V. Kosichkin, A. G. Lyapin et al., J. Non-Cryst. Solids **97–98**, 1459 (1987).

[3] V. F. Degtyareva, I. T. Belash, E. G. Ponyatovskiĭ, and V. I. Rasshchupkin, Fiz. Tverd. Tela (Leningrad) **32**, 1429 (1990) [Sov. Phys. Solid State **32**, 834 (1990)].

[4] J. D. Joannopoulos and G. Lucovsky (eds.), *Physics of Hydrogenated Amorphous Silicon*, Springer-Verlag, New York (1984) [Russian translation: Mir, Moscow (1987), Vol. 1, p. 15].

[5] S. V. Demishev, Yu. V. Kosichkin, D. G. Lunts et al., Zh. Eksp. Teor. Fiz. **100**, 707 (1991) [Sov. Phys. JETP **73**, 394 (1991)].

[6] A. R. Regel' and V. M. Glazov, *Physical Properties of Electronic Melts* [in Russian], Nauka, Moscow (1980), p. 102.

[7] *Handbook of Copper-Based Two-Component and Multicomponent Systems* [in Russian], Nauka, Moscow (1979), p. 14.

[8] A. F. Skryshevskiĭ, *Structural Analysis of Liquids and Amorphous Solids* [in Russian], Vysshaya Shkola, Moscow (1980), p. 47.

[9] M. Essamet, B. Hepp, N. Proust, and J. Dixmier, J. Non-Cryst. Solids **97–98**, 191 (1987).

[10] V. Z. Parton, *Mechanics of Fracture* [in Russian], Nauka, Moscow (1990), p. 80.

[11] S. V. Demishev, Yu. V. Kosichkin, A. G. Lyapin et al., Fiz. Tverd. Tela (Leningrad) **30**, 3691 (1988) [Sov. Phys. Solid State **30**, 2119 (1988)].

[12] B. I. Shklovskiĭ, Zh. Eksp. Teor. Fiz. **72**, 288 (1977) [Sov. Phys. JETP **45**, 152 (1977)].

[13] A. S. Skal, Zh. Eksp. Teor. Fiz. **88**, 516 (1985) [Sov. Phys. JETP **61**, 302 (1985)].

[14] B. Ya. Balagurov, Fiz. Tekh. Poluprovodn. **20**, 1276 (1986) [Sov. Phys. Semicond. **20**, 805 (1986)].

[15] G. Edelin and D. Mathiot, Philos. Mag. B **42**, 95 (1980).

[16] N. F. Mott and E. A. Davis, *Electronic Processes in Non-Crystalline Materials*, Clarendon Press, Oxford (1971) [Russian translation: Mir, Moscow (1982), Vol. 1, p. 66].

[17] T. F. Mazets, É. A. Smorgonskaya, K. D. Tséndin, and V. Kh. Shpunt, *Abstr. of the Second All-Union Conf. on the Physics of Glassy Solids* [in Russian], Riga, November 12–15, 1991, p. 62.

[18] S. V. Demishev, Yu. V. Kosichkin, D. G. Lunts et al., *ibid.*, p. 126.

Translated by Steve Torstveit

1028   Sov. Phys. JETP **74** (6), June 1992

Brazhkin *et al.*   1028